Chapter Four: Laboratory Characterisation of the Aerodyne Aerosol Mass Spectrometer

Laboratory characterisation of the Aerodyne aerosol mass spectrometer has been an important part of this work. At the start of this research project the AMS was a recently developed and poorly understood instrument. A number of research groups within the AMS users community have collaborated by conducting various laboratory experiments; the results of which have significantly contributed to our current understanding of various aspects of the AMS. However, most of these efforts have focused on the AMS response to inorganic aerosols. The majority of the research efforts directed at understanding the ability of the AMS to measure organic aerosols has been conducted as part of the work presented in this thesis. In this chapter, the results of these laboratory experiments are described and discussed.

4.1 Generation of aerosol particles

Particles of known size and composition must be supplied to the AMS to perform various calibrations and laboratory experiments. Polydisperse aerosol particles were generated from solutions using a nebuliser or a collison atomiser [*May, 1973*]. Water and methanol were used as solvents depending on the polarity of the compound of interest, and solution concentrations ranged between 30 – 60 mM. Concentrations were optimised so that the produced number of particles of a desired size is high enough to obtain good AMS signal statistics and low enough to not saturate the electron multiplier detector (typically 200 – 600 p cm^{-3}). Particles generated from the nebuliser were dried using the appropriate drying agent (drierite, silica gel, and activated carbon). A differential mobility analyser (DMA) was then used to select particles of the desired size and produce a near monodisperse sample for analysis. Particle number concentrations were simultaneously measured with the AMS and a condensation particle counter (CPC, TSI model 3025A), mounted upstream of the AMS inlet. The aerosol generation set up is illustrated in Figure 4.1. Unless otherwise stated, monodisperse particles of 350 nm were selected for analysis in all calibrations and laboratory experiments. This size has been selected because particles of this size can be transmitted by the aerodynamic lens with 100% efficiency, and it is within the operating size range of the DMA.

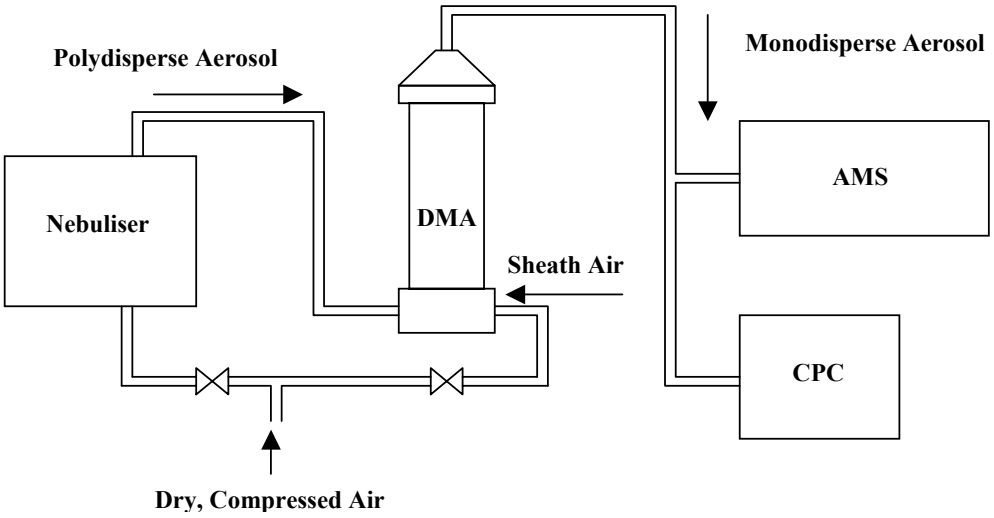

Figure 4.1: Setup for generating Particles of known size and composition

The principles of the CPC and the DMA were described in chapter 2 (sections 2.2 and 2.3, respectively). During the work described in this thesis, the DMA was used as a 'classifier', where a fixed voltage was applied to allow particles of a desired size cut only to pass through. The DMA was calibrated regularly using Polystyrene spheres (PSL) of known sizes to ensure that it selected particles of the correct sizes. In practice the DMA delivers not only particles with the required size but also a small number of particles with multiple and triple charges, which have the same electrical mobility as the singly charged ones. Although particles with multiple and triple charges can affect the total number concentration of particles, they can easily be detected by the AMS during the TOF mode of operation as they have different vacuum aerodynamic sizes.

4.2 Qualitative comparison of AMS and NIST organic mass spectra

The complex mixture of compounds present in ambient aerosol particles makes it unlikely to identify and quantify individual organic compounds using the AMS in its current configuration due to a lack of separation and extensive fragmentation during the electron impact ionisation (see chapter 3, section 3.5). However, for distinguishing different groups of organic compounds, it is crucial to verify that the AMS consistently reproduces mass spectral signatures of organic compounds similar to those produced by a standard 70 eV electron impact ionisation source. A qualitative comparison of organic

fragmentation patterns produced by the AMS with those reported in the NIST library of 70 eV EI spectra will confirm their similarity and help determine any systematic differences that could be used for interpretation of AMS data. The NIST spectra used in this comparison were obtained from the NIST 98 mass spectral search program (version 2.0), which is commonly used by analytical chemists for identification of organic compounds in gas and liquid chromatography – mass spectrometry analysis (GC/LC-MS).

Several organic compounds, representing various functional groups, were selected for this comparison and are listed in Table 4.1, along with their functional groups, molecular weights and formulae. The selection includes compounds of different functional groups such as aromatic and aliphatic hydrocarbons, carbonyls, alcohols, esters and mono-, di-, oxo- and hydroxy- carboxylic acids. Compounds have been selected on the basis of their reported presence in ambient particles [*Seinfeld and Pandis, 1998*], and in a few cases, to investigate the signatures of specific functional groups. The AMS spectra used for this comparison were obtained at vaporiser temperatures between 500 – 550 ^{o}C. This corresponds to the temperatures used in most of the AMS studies to date, and therefore the results of this comparison can be applied to analysis of data in chapters 5, 6 and 7. The effect of the vaporiser temperature on the fragmentation patterns of organic compounds and whether a different temperature would enable better detection of organic compounds is discussed in the next section of this chapter.

Compound	Functional Group	MW	Formula
Myristic acid	Mono-carboxylic acid	228	$C_{14}H_{28}O_2$
Oleic acid	Mono-carboxylic acid	282	$C_{18}H_{34}O_2$
Nonanoic acid	Mono-carboxylic acid	158	$C_9H_{18}O_2$
Decanoic acid	Mono-carboxylic acid	172	$C_{10}H_{20}O_2$
Hexadecanoic acid	Mono-carboxylic acid	256	$C_{16}H_{32}O_2$
Octadecanoic acid	Mono-carboxylic acid	284	$C_{18}H_{36}O_2$
Oxalic acid	Di-carboxylic acid	90	$C_2H_2O_4$
Malonic acid	Di-carboxylic acid	104	$C_3H_4O_4$
Succinic acid	Di-carboxylic acid	118	$C_4H_6O_4$
Glutaric acid	Di-carboxylic acid	132	$C_5H_8O_4$
Adipic acid	Di-carboxylic acid	146	$C_6H_{10}O_2$
Azelaic acid	Di-carboxylic acid	188	$C_9H_{16}O_2$
Pyruvic acid	Oxo-carboxylic acid	88	$C_3H_4O_3$
Benzoic acid, 3-Hydroxy	Hydroxy-carboxylic acid	138	$C_7H_6O_3$
Decanol	Alcohol	158	$C_{10}H_{22}O$
Hexadecanol	Alcohol	242	$C_{16}H_{34}O$
Pyrene	Poly Aromatic Hydrocarbon	202	$C_{16}H_{10}$
Toluene	Aromatic Hydrocarbon	92	C_7H_8
Benzyl Alcohol	Aromatic Hydrocarbon	108	C_7H_8O
Nonylaldehyde	Aldehyde	142	$C_9H_{18}O$
Decylaldehyde	Aldehyde	156	$C_{10}H_{20}O$
2-Nonanone	Ketone	142	$C_9H_{18}O$
Methyl glyoxal	Oxo-aldehyde	72	$C_3H_4O_2$
p-Nitro Phenol	Nitro, Hydroxy Aromatic	139	$C_6H_5NO_3$
Urea	Di-amine	60	CH_4N_2O
DOS	Ester	426	$C_{26}H_{50}O_4$
Decane	Saturated Hydrocarbon	142	$C_{10}H_{22}$

Table 4.1: A list of organic compounds used to compare AMS and NIST spectra

A qualitative comparison of AMS and NIST mass spectra demonstrated that the investigated organic compounds could be classified into three groups. The first group of compound showed AMS mass spectra nearly identical to those reported in NIST. This group included mainly compounds with aromatic ring structures. Aromatic hydrocarbons have been reported as precursors for secondary aerosol formation [*Forstner et al., 1997; Odum et al., 1997*], while polycyclic aromatic hydrocarbons (PAHs) were one of the first atmospheric species to be identified as being carcinogenic [*Seinfeld and Pandis, 1998*]. Figure 4.2 shows an AMS mass spectrum of the PAH, pyrene, and the equivalent NIST mass spectrum, and a similar comparison of p-nitrophenol spectra is shown in Figure 4.3. The spectra reveal that little fragmentation of parent molecular ions is observed. This is attributed to the stability of the molecular ions due to the ring system. This stability explains the fewer mass fragments of pyrene (4 rings) compared to 4-nitrophenol (1 ring).

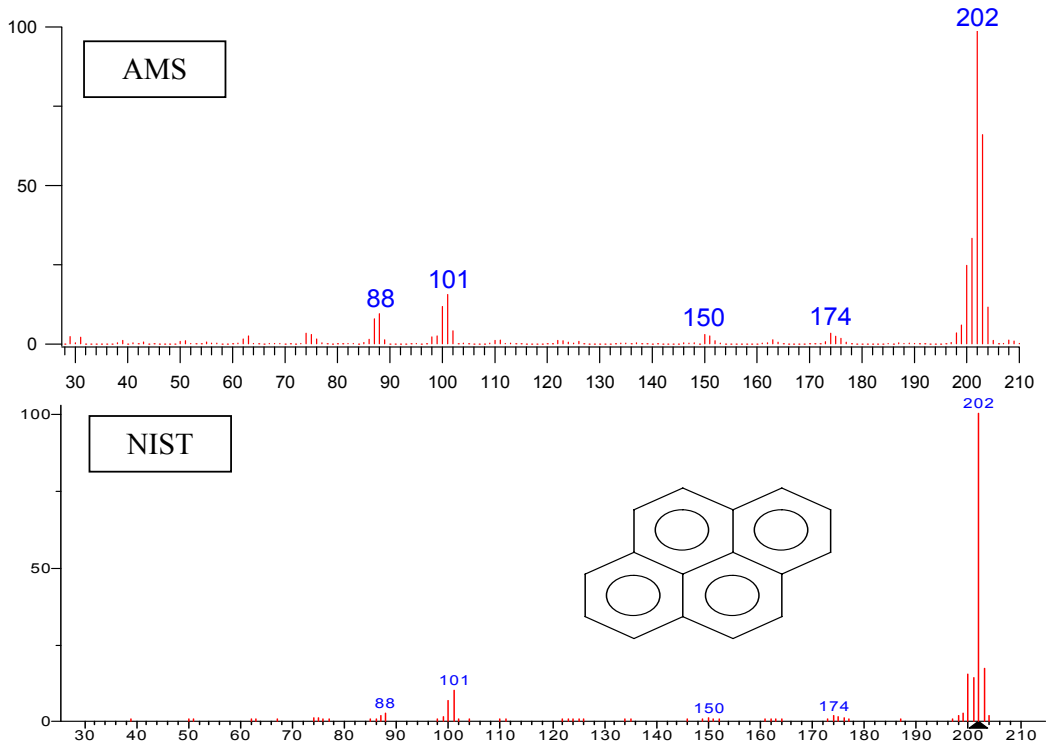

Figure 4.2: Comparison of AMS and NIST mass spectra for pyrene

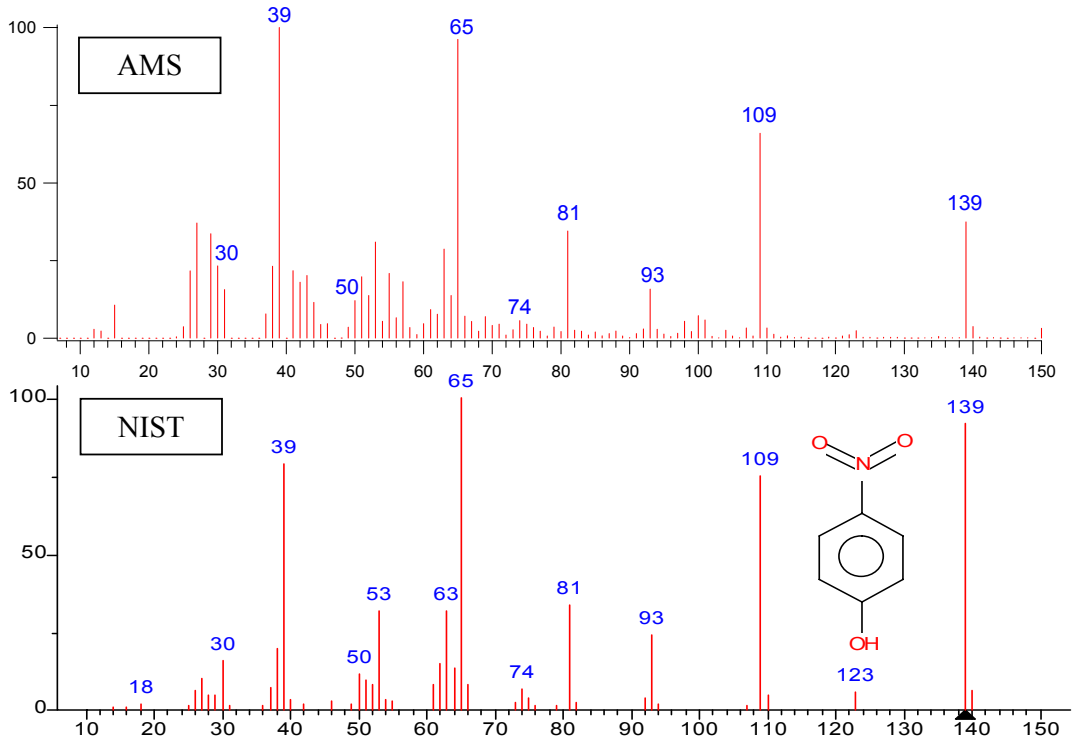

Figure 4.3: Comparison of AMS and NIST mass spectra for p-nitrophenol

The second group of compounds showed consistent AMS spectra with NIST, in terms of most of the observed ion fragments. However, the relative intensities of the ion fragments were different. In general, smaller ion fragments (< *m/z* 60) appear to be more intense in AMS spectra, while the opposite was observed for higher masses. The observed difference between the AMS and NIST spectra indicates that the AMS vaporisation and ionisation configuration results in a more significant fragmentation of long chain species than in the case of standard electron impact ionisation mass spectrometry. The studied group of compounds included long chain species with several functional groups such as saturated hydrocarbons, monocarboxylic acids, esters, alcohols and carbonyls. Long chain species are commonly measured in ambient aerosol particles, and arise from both combustion and natural vegetation sources. Examples of the AMS and NIST mass spectra of myristic acid (tetradecanoic acid) and hexadecanol are shown in Figures 4.4 and 4.5, respectively. The spectra illustrate the typical significant fragmentation of long chain species in an electron impact ionisation source. Most of the observed mass fragments can be accounted for by the two hydrocarbon related ion series, C_nH_{2n+1} and C_nH_{2n-1} (e.g. *m/z* 27, 29, 41, 43, 55, 57).

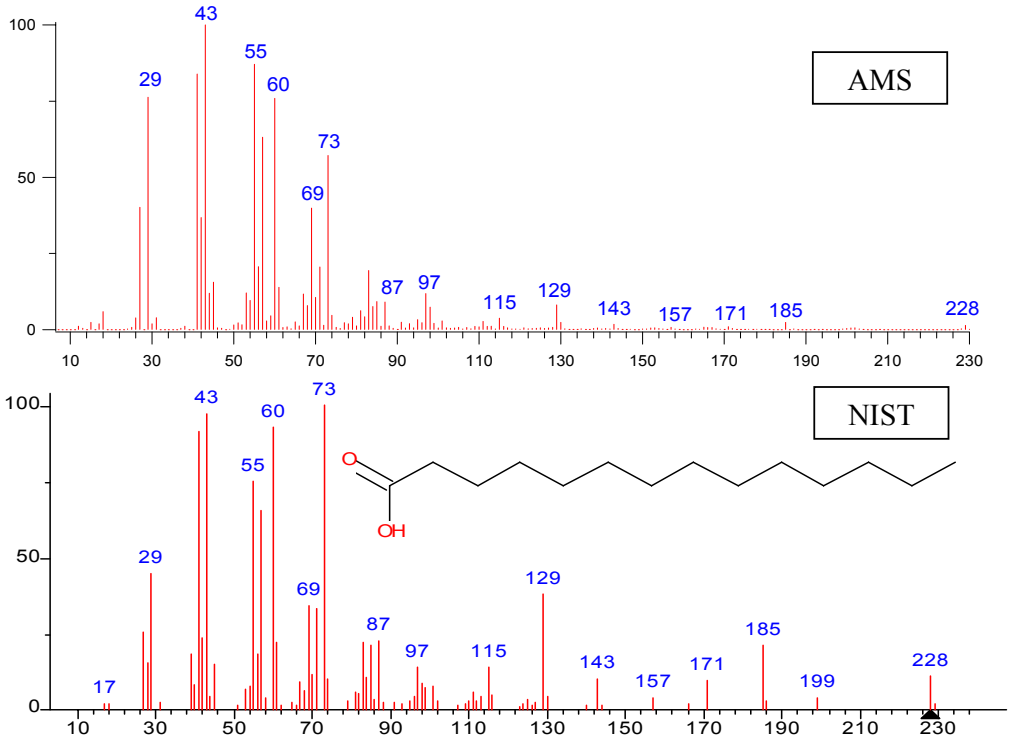

Figure 4.4: Comparison of AMS and NIST mass spectra for myristic acid

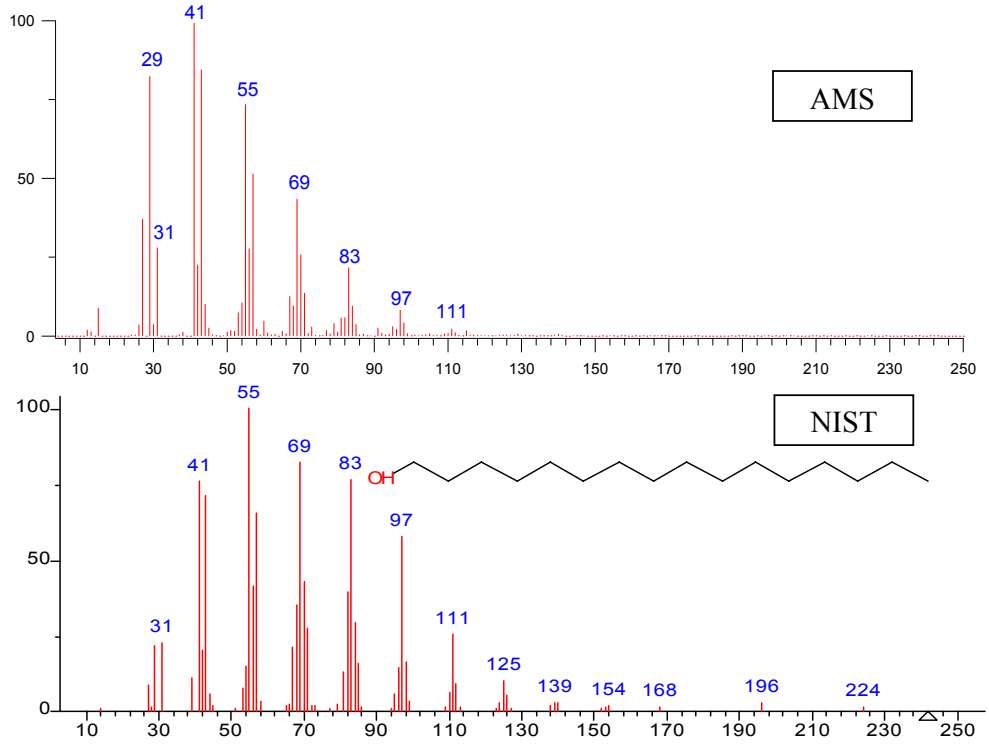

Figure 4.5: Comparison of AMS and NIST mass spectra for hexadecanol

The AMS spectra of the third group of compounds showed, in addition to the mass fragments reported in NIST, two consistent and significant mass fragments that were absent or showed very low abundance in the equivalent NIST spectra. The two mass fragments are 18 and 44 corresponding to the parent ions of water (H_2O^+) and carbon dioxide (CO_2^+), respectively. This characteristic feature was observed in the mass spectra of most oxidised compounds, exhibiting high polarity, in Table 4.1. Oxidised compounds, such as hydroxy-, oxo- and di-carboxylic acids have been widely reported as secondary organic aerosol products that are formed from the photooxidation of volatile organic compounds [*Forstner et al., 1997; Larsen et al., 2001; Jaoui and Kamens, 2003; Kleindienst et al., 2004*]. In Figure 4.6 the AMS mass spectrum of oxalic acid is shown in comparison to the equivalent NIST spectrum. It is immediately apparent that mass fragments 18 (H_2O^+) and 44 (CO_2^+) dominate the AMS spectrum, while all of NIST peaks can still be observed (with the exception of *m/z* 28 due to interference from ambient N_2^+ ions).

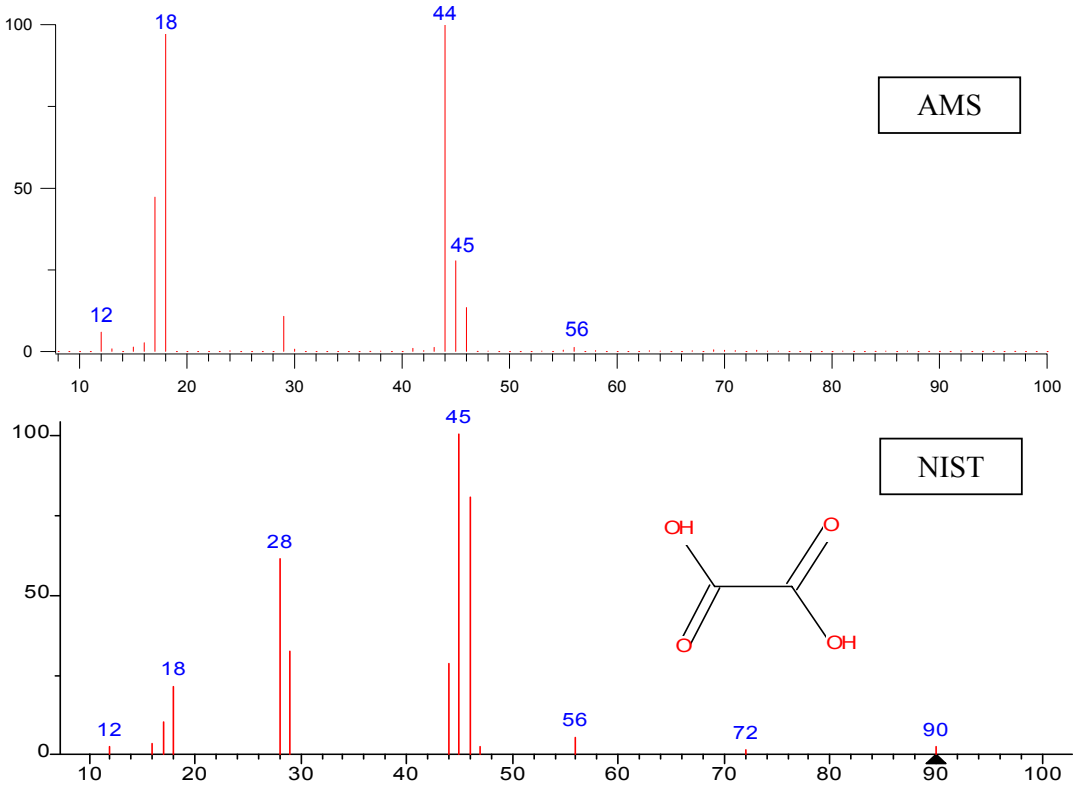

Figure 4.6: Comparison of AMS and NIST mass spectra for oxalic acid

The presence of mass fragments 18 and 44 in the AMS mass spectra of highly oxidised compounds appears to represent a systematic difference between the AMS and NIST data. The significant presence of H_2O^+ and CO_2^+ in the AMS data could be an indication of thermal decomposition of highly oxidised compounds due to the elevated vaporiser temperature. It is important to note that the NIST data was acquired from compounds already present in the gas phase using an EI ion source typically at 250 ^oC. On the other hand, the AMS data is obtained by flash vaporisation of solid or liquid particles on a 500 ^oC heated surface. It is possible that the ion fragment CO^+ (*m/z* 28) may also result in this process and is dwarfed by the ambient N_2^+ ions at the same *m/z*. The fragmentation patterns of highly oxidised compounds could be investigated by generating aerosol particles using an inert gas (e.g. argon) instead of compressed air. It was not possible to carry out this experiment due to the long absence of the AMS on field projects. Similar experiments have been performed in another laboratory, although the results have not yet been published [*P. Silva, Utah State University, Personal Communication*].

The AMS mass spectra for the remaining compounds in Table 4.1 and the equivalent NIST spectra are shown in Appendix 2. In summary, the data illustrate that the AMS mass spectra are qualitatively similar to NIST spectra. However, two systematic differences have been observed between the two sets of data. Firstly, more fragmentation of long chain species tends to occur in the AMS data. Secondly, mass fragments arising due to thermal decomposition of highly oxidised organic compounds have been uniquely observed in the AMS spectra. These two differences are likely to be caused by the same mechanism, since lower mass fragments are typically produced as a result of thermal decomposition. The differences in the intensities of ion fragments produced from long chain species between the AMS and NIST data do not prevent the utilisation of NIST data in the interpretation of AMS ambient data. This is because it only shifts the relative intensities of the ion fragments in the AMS spectra compared to NIST without introducing any new ion fragments. On the other hand, the formation of the decomposition mass fragments H_2O^+ and CO_2^+, uniquely from highly oxidised organic compounds in the AMS and their absence from NIST data, is of much greater importance in interpreting ambient AMS data since they can be used to determine the

degree of oxygenation of ambient aerosol particles. However, only the CO_2^+ signal at *m/z* 44 can be used quantitatively in ambient data. This is because the H_2O^+ signal at *m/z* 18 receives contribution from gas phase water, and since ambient humidity varies with time and location, it would be difficult to measure the organic contribution to *m/z* 18. On the other hand, the uniform gas phase concentration of CO_2 enables the subtraction of its contribution to *m/z* 44 in the mass spectrum and allows for quantitative detection of the organic-related CO_2^+ in ambient data.

4.3 Investigation of the effect of the vaporiser temperature on the detection of inorganic and organic compounds

The separation of the vaporisation and ionisation processes is a fundamental step in achieving quantitative AMS measurements (see chapter 3, section 3.1.3). Therefore, the vaporiser temperature has to be optimised to be as high as necessary to ensure full vaporisation of particles, and as low as possible to avoid surface ionisation resulting in ions, which are difficult to quantify and also to limit the increased fragmentation that appears to occur relative to standard gas phase EI for many organic compounds. Experiments have been conducted to investigate the effect of the vaporiser temperature on the detection of inorganic salts, commonly measured in ambient particles, such as ammonium nitrate and ammonium sulphate as well as a number of organic compounds representing various classes.

Experiments were carried out by generating volatile and semi-volatile aerosol particles of known size and composition using the setup described in Figure 4.1. Mass spectra and TOF data were collected for each compound at seven heater temperature settings between 300 ^oC and 750 ^oC. Results are reported as the number of ions generated per particle (IPP) plotted as a function of vaporiser temperature. The IPP were calculated by summing up all ions detected at each *m/z* channel from the mass spectral data, subtracting gas phase contributions and dividing by the total number of particles counted by the AMS. This ratio was multiplied by the fraction of number of singly charged particles to the total number of particles counted by the AMS from the TOF data to ensure that all calculations are being performed to the singly charged particles of the desired size cut set by the DMA and excludes contribution form multiple and triplet

charged particles. This calculation also accounts for any variability in the number of particles delivered into the AMS. The vaporiser temperature was measured by a built-in thermocouple, and was set manually by controlling the power supply to the vaporiser. Figure 4.7 shows the corresponding vaporiser temperatures, in ^{o}C, for a range of power values, in watt. The observed offset in temperature when no power was supplied is due to thermal radiation from the ion source (the filament).

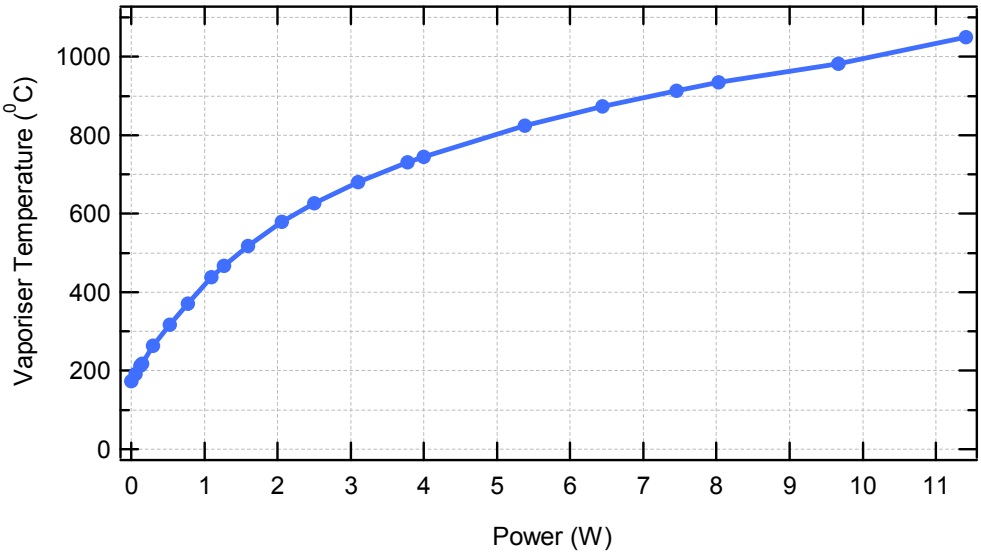

Figure 4.7: Vaporiser temperature as a function of vaporiser power

The effect of the vaporiser temperature on the detection of nitrate and sulphate ions (produced from their respective ammonium salts) is illustrated in Figure 4.8. Increasing the vaporiser temperature up to 500 ^{o}C appears to have a more significant effect on the detection of sulphate ions compared to nitrate ions. The results show that vaporiser temperatures below 500 ^{o}C are not high enough to fully vaporise ammonium sulphate and, to a lesser extent, ammonium nitrate particles and therefore, result in the underestimation of measured mass concentrations of these components. In addition, low vaporiser temperatures may cause slow vaporisation of particles, resulting in broad size distributions and possible interferences among time of flight cycles. On the other hand, the detection of nitrate ions seem to decrease at vaporiser temperatures higher than 600 ^{o}C, with no significant effect on sulphate ions over this range of temperatures. The difference in the effect of vaporiser temperatures on the detection of nitrate and sulphate

ions may be explained by the fact that ammonium sulphate particles are less volatile than ammonium nitrate.

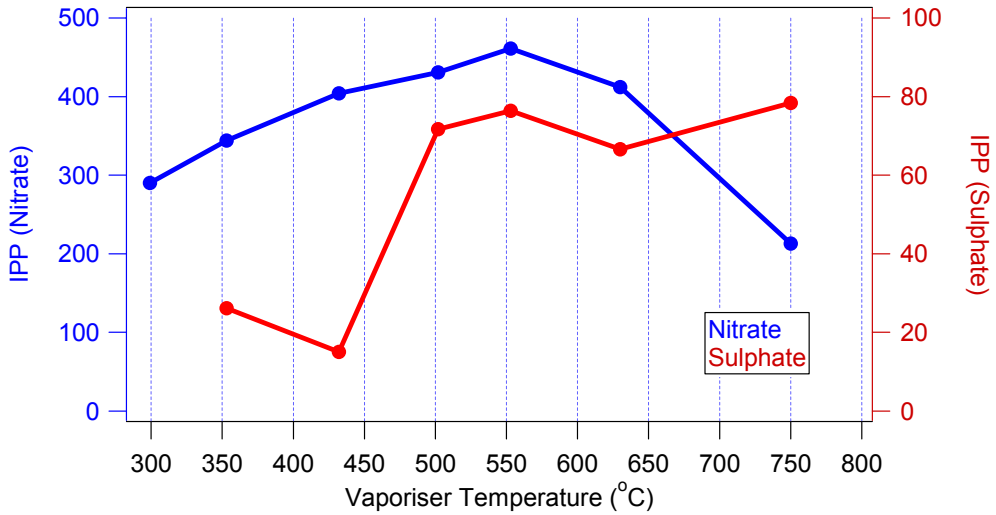

Figure 4.8: Effect of the vaporiser temperature on the detection of nitrate and sulphate ions

Similar experiments have been performed to investigate the effect of the vaporiser temperature on the detection of a number of organic compounds, representing various functional groups. The effect of vaporiser temperature on the total detected ions per organic particle has been studied. However, since EI ionisation results in more fragmentation of organic compounds relative to inorganic salts, additional analyses have been performed to inspect the effect of vaporiser temperature on the detection of organic mass fragments classified on the basis of their molecular weight. The mass spectrum of each compound has been divided into three sections containing low, medium and high mass fragments (simply by dividing the molecular weight of each compound by 3). The IPP for each section were calculated as described above and plotted on each graph along the total IPP. Figure 4.9 illustrates an example of the calculated IPP as a function of vaporiser temperature for oleic acid.

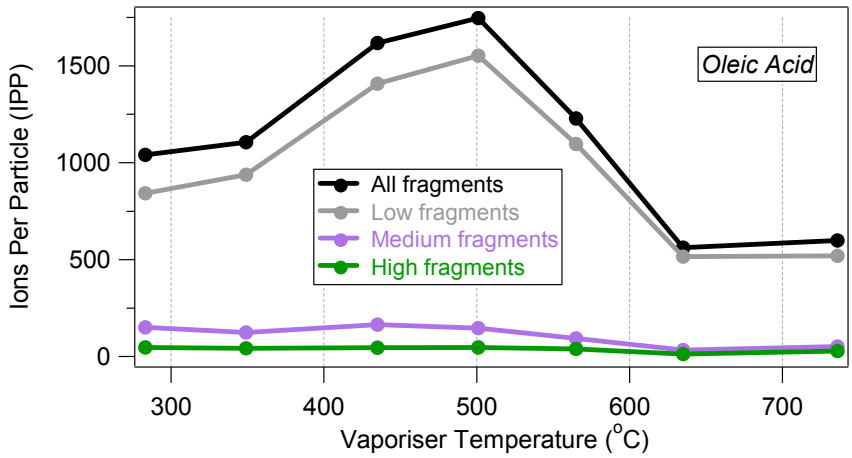

Figure 4.9: Effect of the vaporiser temperature on the detection of oleic acid ions

The results of all studied compounds have been consistent and have shown similar behaviour of the detected ions per particle as a function of vaporiser temperature. Low vaporiser temperatures (< 400 ^{o}C) appear to cause incomplete vaporisation of particles due to insufficient thermal energy and result in the detection of low IPP. Increasing the vaporiser temperature up to about 500 – 550 ^{o}C seemed to maximise the detected IPP for all studied compounds. The detected IPP decreased as vaporiser temperature exceeded 550 – 600 ^{o}C. To date, there is no clear explanation of what appears to be a systematic decrease in IPP values at high vaporiser temperatures. However, the results clearly show that the vaporiser temperature has to be carefully chosen to ensure optimum detection of organic compounds. Figure 4.10 shows that compounds like myristic acid, pyrene and di-octylsabacate (DOS) have a plateau of temperatures over which maximum IPP values can be detected. On the other hand, other compounds like nonylaldehyde, p-nitrophenol and succinic acid seem to produce their maximum IPP values at around 500 ^{o}C (Figure 4.11). The results of the investigated inorganic and organic compounds suggested that a vaporiser temperature in the range of 500 – 550 ^{0}C would result in the maximum possible detection of ions. This range of temperatures has been used in all of the AMS studies reported in this thesis. The effect of this vaporiser temperature on the fragmentation patterns of organic compounds and a comparison with fragmentation patterns of organic compounds in the NIST library of EI spectra has been discussed in section 4.2.

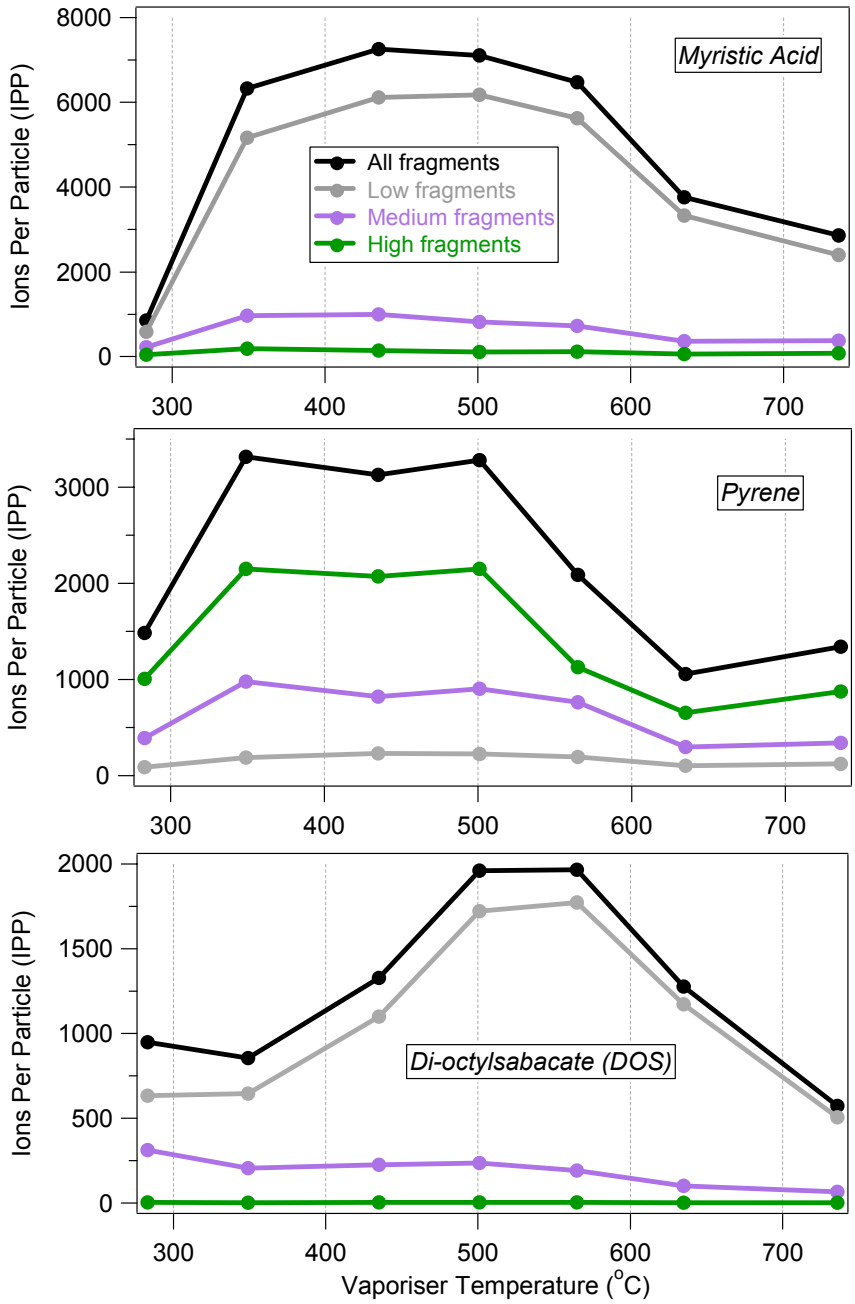

Figure 4.10: Effect of the vaporiser temperature on the detection of myristic acid, pyrene and di-octylsabacate (DOS) ions, repectively.

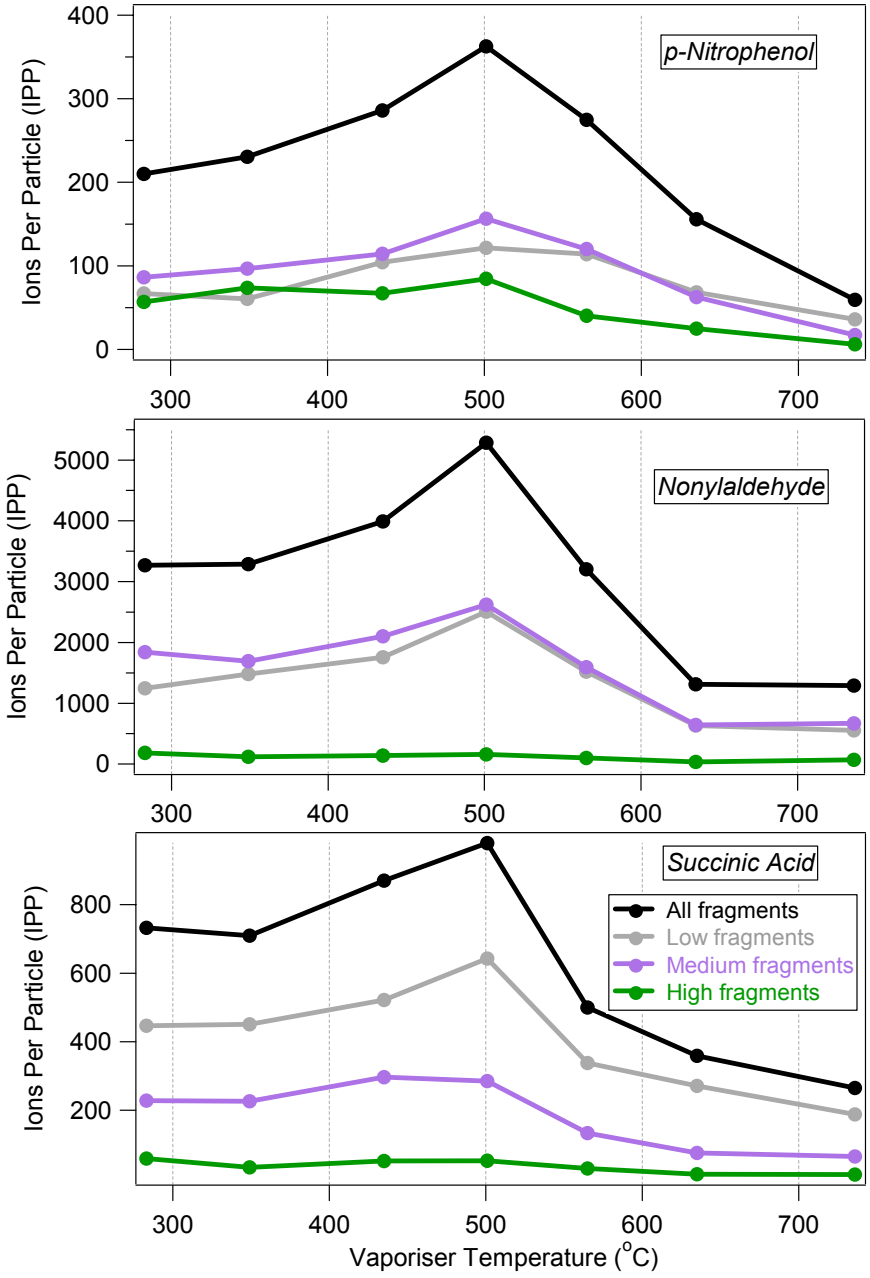

Figure 4.11: Effect of the vaporiser temperature on the detection of p-nitrophenol, nonylaldehyde and succinic acid ions, repectively.

4.4 AMS collection efficiency of organic aerosol particles

Particle collection efficiency, *CE*, is defined as the fraction of sampled particle mass that is detected by the AMS [*Alfarra et al., 2004*]. The need to define particle collection efficiency and how it is used in calculating AMS mass concentrations has been discussed in chapter 3 (see section 3.3). Particle collection efficiency can be measured, for particles of known size and composition, by comparing the number of particles counted simultaneously by the AMS and a condensation particle counter (CPC). An AMC/CPC ratio close to 100% means that the AMS is detecting and counting all available particles, while lower ratios indicate lower AMS collection efficiency.

There are two main factors that determine the AMS particle collection efficiency. The first factor is the aerodynamic lens particle transmission efficiency, which is a function of particle size [*Liu et al., 1995a; Liu et al., 1995b*]. The current AMS lens can transmit particles in the vacuum aerodynamic diameter range from 30 up to 650 nm with near 100% efficiency, as described in section 3.1.1. The lens transmission efficiency has also been reported to be a function of particle shape [*Liu et al., 1995a; Liu et al., 1995b*]. Spherical particles appear to be transmitted with near 100% efficiency, while particles with irregular shapes seem to be transmitted with much lower efficiency. The second factor that determines AMS particle collection efficiency is the volatility of particles. The AMS has been designed to detect the non-refractory fraction of aerosol particles, where non-refractory is an operational definition for particles that can be vaporised at the applied vaporiser temperature. It is also possible that particles bounce away from the vaporiser occurs before vaporisation can take place. Therefore, the AMS collection efficiency for ambient particles is a function of particle size, shape and volatility. An experiment has been carried out to evaluate the AMS particle collection efficiencies for six volatile and semi-volatile organic compounds. In order to limit the variables controlling the AMS particle collection efficiency to particle shape only, 350 nm particles only have been studied and the AMS vaporiser temperature has been set to 500 ^{o}C, as suggested from the results is section 4.3.

The results obtained for the six organic compounds are shown in Figures 4.12 and 4.13, where the number of counted particles (p cm^{-3}) is plotted on the Y-axis and the mass

fragments scanned in the TOF mode for each compound are plotted X-axis. Each graph shows the average total particle number density as counted by the CPC, and the average number density of total particles as well as singly charged particles as counted by the AMS at each selected mass fragment. The difference between the numbers of the total and singly charged particles is useful to estimate the number of multiple and triplet charged particles that have the same mobility diameter as the singly charged ones. The results have shown that the six compounds can be classified into two groups. The first group includes oleic acid, nonylaldehyde and di-octylsabacate (DOS) and they have all been collected with near 100% efficiency, as shown in Figure 4.12. On the other hand, the second group of compounds have been collected with only 20 to 50% efficiencies, as illustrated in Figure 4.13.

Interestingly the first group of compounds, *CE* ~ 100%, were all originally liquids, while the second group with reduced collection efficiencies were originally solids. These measurements and the reported optimum lens transmission efficiency for spherical particles and reduced transmission of irregularly shaped particles may support the claim that liquid compounds generally produce spherical particles, while solid compounds mostly produce particles, which are irregular in shapes. A further explanation may be that liquid particles spread or splash on impact and are readily vaporised whereas solid particles can bounce away from the vaporiser. This observation has been supported by the near 100% collection efficiency of ammonium sulphate particles when sampled at 90% relative humidity compared to less than 20% collection of ambient ammonium sulphate particles [*Allan et al., 2004a*].

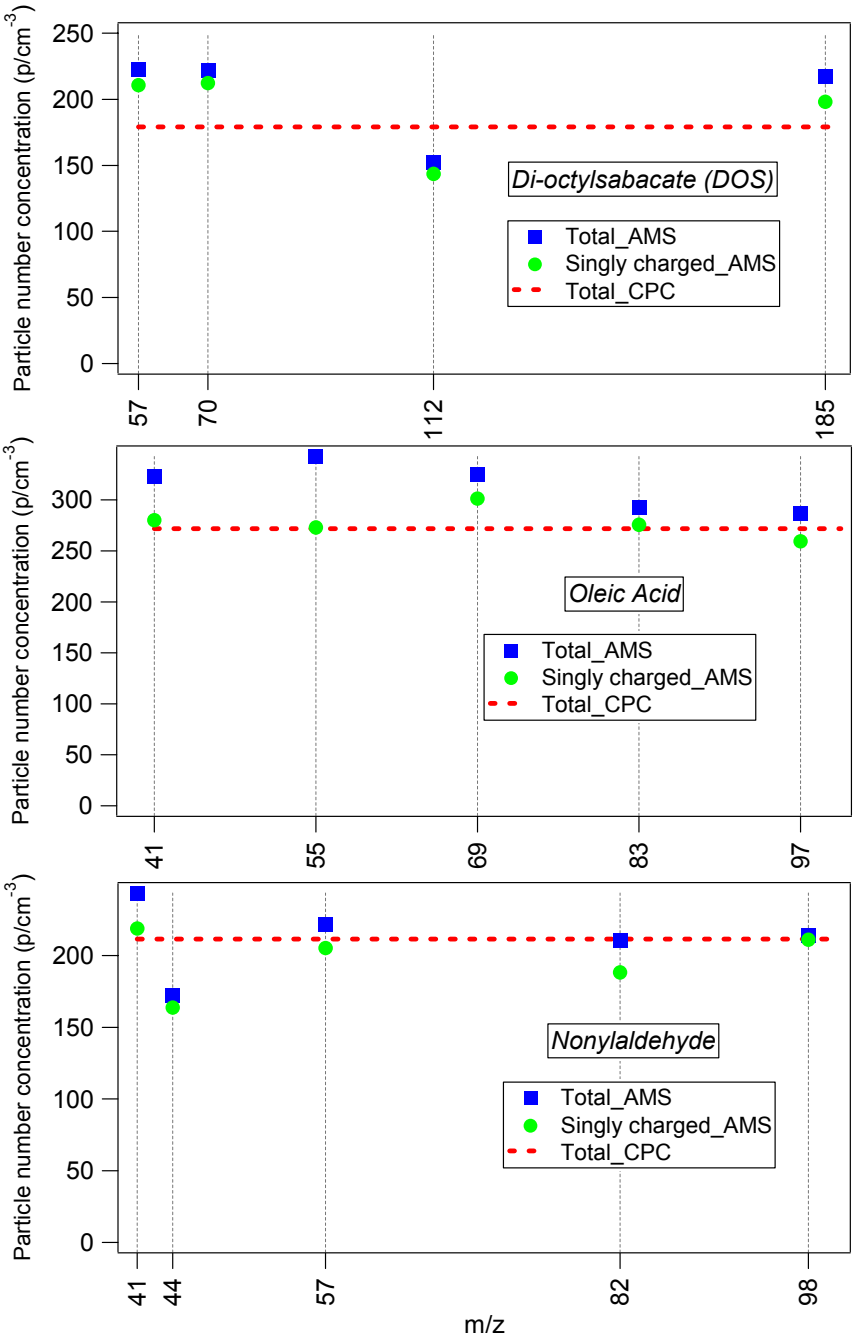

Figure 4.12: AMS collection efficiency for DOS, oleic acid and nonylaldehyde, respectively

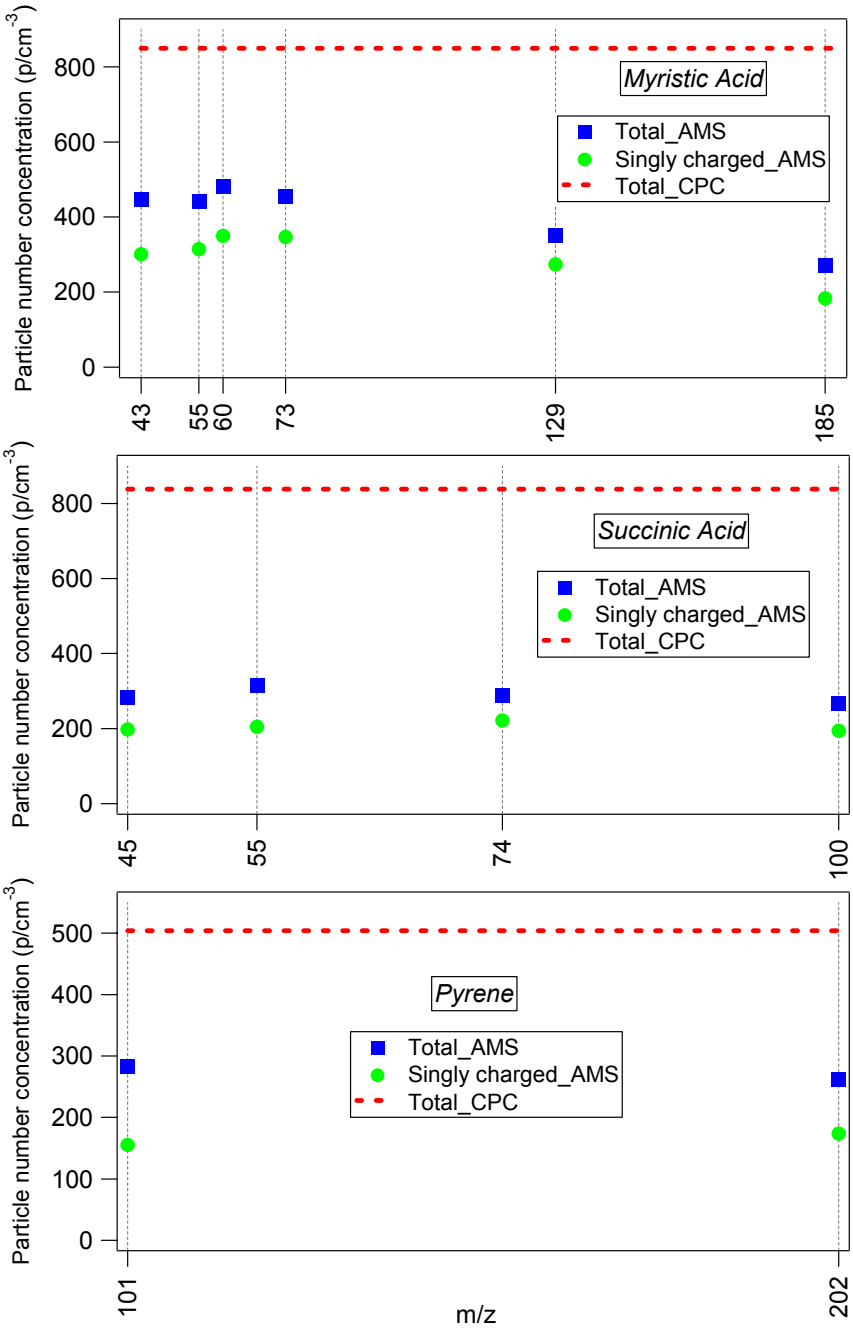

Figure 4.13: AMS collection efficiency for myristic acid, succinic acid and pyrene, respectively

4.5 Fragmentation ratios of nitrate salts

Inorganic salts produce typically simple mass spectra containing a few fragments. For instance, the nitrate ions (NO_3^-) from ammonium nitrate particles tend to produce two main fragments, NO^+ at *m/z* 30 and NO_2^+ at *m/z* 46. Since various nitrate salts exist in ambient particles, an experiment has been performed to measure the NO^+/ NO_2^+ ratios of four different nitrate salts, including ammonium nitrate (NH_4NO_3), sodium nitrate $NaNO_3$, calcium nitrate $Ca(NO_3)_2$ and magnesium nitrate $Mg(NO_3)_2$. Particles were generated from aqueous solutions and AMS mass spectra of all compounds were acquired for 350nm particles. The ratios of *m/z* 30 to *m/z* 46 for each salt are shown in Table 4.2. The results suggest that, after ruling out any other possible interference from other chemical species, the NO^+/ NO_2^+ ratio can be used as an indication of the type of nitrate salt measured in ambient particles.

Compound	NO^+/ NO_2^+
NH_4NO_3	2.7
$Mg(NO_3)_2$	10.6
$NaNO_3$	29.2
$Ca(NO_3)_2$	45.6

Table 4.2: Ratios of NO^+/ NO_2^+ (mz 30/ mz 46) fragments produced by different nitrate salts